

Solar Filaments as Tracers of Subsurface Processes

D. M. Rust, *Applied Physics Laboratory, Johns Hopkins University, 11100 Johns Hopkins Road, Laurel, MD 20723, USA.*
e-mail: david.rust@jhuapl.edu

Abstract. Solar filaments are discussed in terms of two contrasting paradigms. The standard paradigm is that filaments are formed by condensation of coronal plasma into magnetic fields that are twisted or dimpled as a consequence of motions of the fields' sources in the photosphere. According to a new paradigm, filaments form in rising, twisted flux ropes and are a necessary intermediate stage in the transfer to interplanetary space of dynamo-generated magnetic flux. It is argued that the accumulation of magnetic helicity in filaments and their coronal surroundings leads to filament eruptions and coronal mass ejections. These ejections relieve the Sun of the flux generated by the dynamo and make way for the flux of the next cycle.

Key words. Solar filaments—solar dynamo—magnetic fields.

1. Introduction

Filaments are clouds of relatively cool and dense gas in the solar atmosphere. The Standard paradigm of filament formation invokes condensation of plasma from the corona into dimpled magnetic fields, which are usually supposed to be twisted by shearing and reconnection of existing loops in the corona driven by surface motions. There is, however, a new paradigm about filaments, and twisted fields in general, according to which, probably all the magnetic flux that emerges into the photosphere is twisted. Twisted flux forms sunspots, active regions (ARs) and filaments. The twist accumulates in filaments and coronal arcades. Eventually the accumulated, highly-twisted fields become unstable and erupt. From a study of filament magnetic fields and filament eruptions, then, one might hope to discover important properties of the subsurface processes of the solar dynamo.

2. General properties of filament magnetic fields

The magnetic fields in filaments are nearly horizontal and generally exhibit a helical structure inside an arcade of coronal loops (Athay *et al.* 1983, Rust & Kumar 1994). Fig. 1 is a sketch of an idealized twisted-field filament and its magnetic arcade. The orientation of the axial fields in polar crown filaments, those generally above 50° latitude, shows a distinct dependence on the solar cycle (Leroy *et al.* 1983, Martin *et al.* 1992). In the years leading up to the maximum of even-numbered cycles, for example, the magnetic vectors in polar crown filaments point westward in the

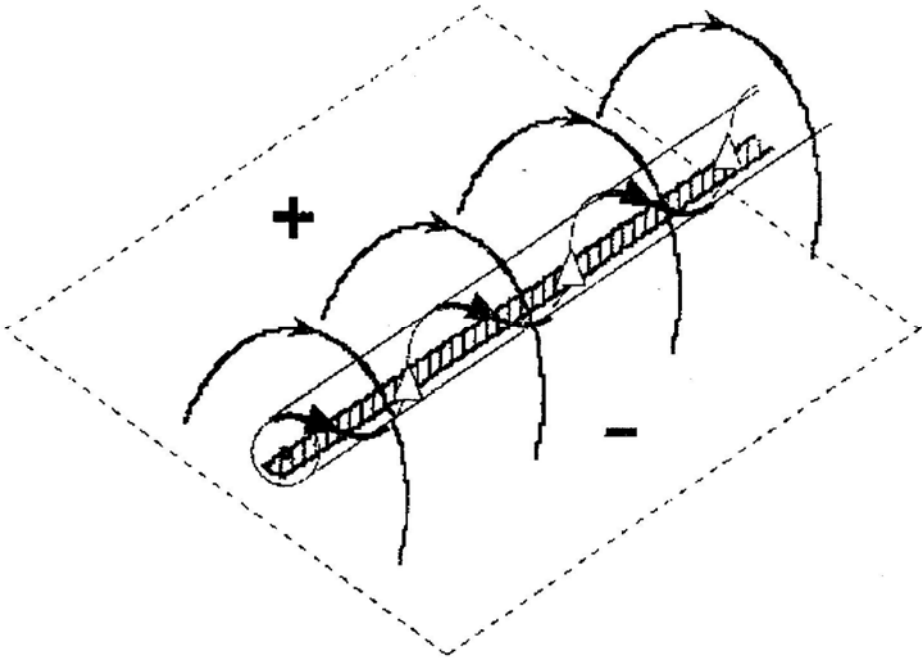


Figure 1. Perspective view of a filament (hatched strip) trapped in a twisted magnetic flux rope. An arcade of coronal loops encloses the filament. Filaments invariably lie on the borders separating positive and negative photospheric fields as shown here.

northern hemisphere and eastward in the southern hemisphere. Thus, these filaments collectively might be thought of as forming two magnetic toroids around the Sun, north and south with a flux of about 10^{20} Mx in each hemisphere. The filaments in ARs also generally follow the same pattern: they extend from a 'leader' spot eastward to a 'follower' spot or to non-spot fields of the same polarity as follower spots, so they could be viewed as segments of toroids as well.

Beginning 4–5 yrs after the onset of each cycle, an increasing number of filaments appears at mid-latitudes, i.e., 30° – 45° . These are the so-called 1st tier or between-AR filaments. Their axial fields point eastward in the northern hemisphere and westward in the southern hemisphere in even-numbered cycles, i.e., they are opposite the fields in the polar-crown and AR filaments (Tang 1987).

First-tier filaments may be related to a peculiar feature of the solar dynamo. Stix (1976) published numerical solutions from a typical dynamo model that suggest that each cycle begins with toroidal fields at latitudes of 35° to 40° . We can identify the fields in the ARs of the cycle with these toroids. But the dynamo also produces weaker, reversed toroids about five years after the onset of the cycle. These toroids strengthen gradually for several years, all the while staying at latitudes above 35° . Thus, their behavior is similar to that of 1st-tier filaments, which also maintain a nearly constant mean latitude, ca. 50° , through most of the cycle. Toward solar minimum, these reversed toroidal fields strengthen and become the source of the ARs of the next cycle. Thus, the patterns of the toroidal fields in normal AR filaments and 1st-tier filaments are consistent with some features of the model of the solar dynamo. First-tier filaments may be the earliest sign of the next solar cycle.

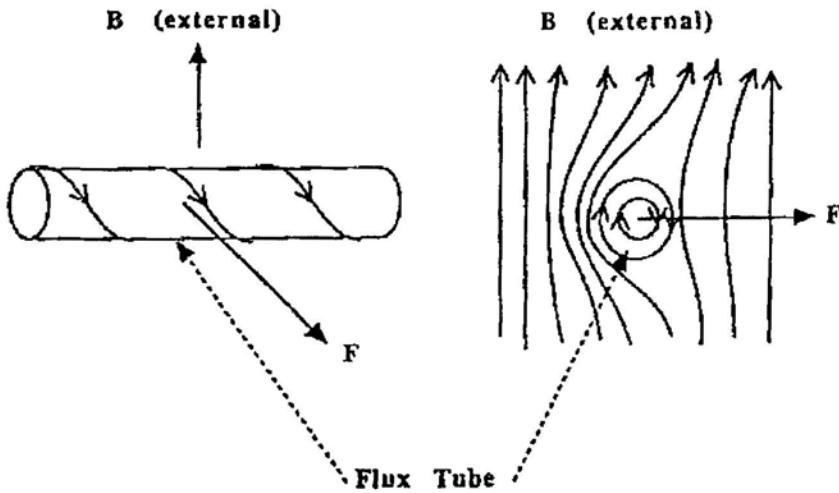


Figure 2. A horizontal flux rope in vertical external fields experiences a force F that is repulsive on one side and attractive on the other.

Twisted horizontal fields thrown up by the dynamo should collect at polarity boundaries. As shown in Fig. 2, there is a lateral force on a horizontal flux rope surrounded by vertical fields. If the flux rope has a net current flowing along its axis, the Lorentz force acting on it, in the presence of an external field will force the flux rope to move until it reaches a polarity boundary, where the horizontal force vanishes. Thus, weak-field horizontal flux ropes will be in stable equilibrium and they will collect at polarity boundaries.

3. Global pattern of filament helicity

Filaments resemble twisted ropes, giving inspiration to the flux rope model (Low & Hundhausen 1995, Amari *et al.* 1999, Rust & Kumar 1994). The recent model of Aulanier & Demoulin (1998) and Aulanier *et al.* (1998) now seem to account quite convincingly for the barbs on filaments in terms of a helical flux rope model distorted by underlying fields. The chirality of the twist, left-handed in the north and right-handed in the south, is consistent with an origin in the dynamo.

Evidence that filaments erupt as the result of an instability in a twisted flux rope was obtained with the X-ray telescope aboard the Yohkoh satellite. A sigmoid (S-shaped) brightening usually appears in X-rays at the onset of filament eruption. The ratio R of sigmoid length to width in a large sample of eruptives peaks at $R = 5$ (Rust & Kumar 1996). This is exactly the ratio of the most likely helical kink instability in a twisted magnetic field. Furthermore, most sigmoid brightenings in the southern hemisphere are S-shaped, as predicted for a helical instability in a field with right-handed twist. Sigmoid brightenings in the north are usually mirror image (reversed) S-shaped, as expected for instabilities in left-handed flux ropes.

Despite some sophisticated calculations (Van Ballegooijen *et al.* 1998), models based on surface motions have not yet explained the global pattern of filament axial fields in the polar crown and in the first tier of filaments. The basic problem is that

differential rotation, which is the only systematic surface motion outside ARs, will shear coronal arcades so that, in even-numbered cycles, the magnetic field vectors in polar crown filaments point eastward in the northern hemisphere and westward in the southern hemisphere, contrary to observations.

Mackay *et al.* (1998) combine surface motions and emergence of twisted flux ropes to show how first tier filaments might form with the required negative helicity in the north and positive helicity in the south. But the key ingredient in their model is the correct helicity of the emergent flux.

If surface motions cannot reproduce the observed toroidal and helical field patterns, then -we can turn to subsurface motions. Suppose that filament fields originate in AR flux ropes and accumulate in the chromosphere and corona. Then the problem becomes one of showing how the AR fields are twisted. Longcope *et al.* (1999) consider how much twist could be imparted by the Coriolis force acting during a flux rope's flight from the base of the convection zone to the photosphere. They conclude that the effect would produce an average twist in ARs at least an order of magnitude lower than that observed by Pevtsov *et al.* (1995). Similarly, they find that subsurface differential rotation falls short by an order of magnitude. They develop a model of subsurface twist imparted by turbulent motions in the convection zone that they call the Σ -effect and that, according to them, could produce the observed average twist in AR fields. They do not consider surface motions, but their Σ -effect model is the first attempt at a quantitative correspondence between the observed amount of helicity on the Sun and plausible subsurface motions.

The amount of helicity K injected into the solar atmosphere by AR fields in each solar cycle can be estimated from the number N of active regions, each with an average flux ϕ and twist per unit length q . Taking $N = 3000$ ARs per cycle, $\phi = 10^{21}$ Mx per AR, $q = 0.02$ rad Min^{-1} as measured by Pevtsov *et al.* (1995), then we find $K = 1.3 \times 10^{45}$ Mx^2 per solar cycle. This is nearly the same value escaping the Sun as estimated by Bieber & Rust (1995) from interplanetary magnetic field (IMF) measurements and from estimates of the helicity in filaments and coronal arcades. Thus it is plausible that the helicity emerging in ARs accumulates in filaments and coronal arcades. As shown in Parker's (1979) book, the twist in an emerged flux rope will migrate into the emerged portion of the rope.

Now that there is so much data on the distribution and quantity of magnetic helicity in the solar atmosphere (Brown *et al.* 1999), it is important to calculate the magnetic helicity from dynamo models. Gilman & Charbonneau (1999) pointed out that most dynamo theories can only calculate the mean fields and helicity that might occur at the base of the convection zone. They say nothing about what might happen to the fields as they rise to the visible surface, but it is useful to review dynamo results here because important features of the predicted cyclic behavior and helicity patterns should be preserved when the fields emerge at the photosphere.

Gilman & Charbonneau (1999) computed mean field strengths for the toroidal and poloidal components and the mean positive and negative current helicity produced by a variety of dynamo models. Current helicity has the same sign as magnetic helicity (Seehafer 1990), so current helicity calculations are useful to see if a realistic dynamo model can reproduce the observed magnetic helicity pattern. Gilman & Charbonneau (1999) computed the helicity from a 'flux transport' model developed by Dikpati & Charbonneau (1999). It is similar to Babcock's (1961) original model of the sunspot cycle. The results are in good general agreement with observations since the toroidal

component is much stronger than the radial component. And while negative (positive) helicity dominates in the north (south), each hemisphere has mixed helicities in the sunspot zones, also in agreement with observations. There is an interesting pattern of added helicity near the poles, and this may be due to the fact that the model does not account for flux escape from the Sun.

Parker (1984) and Vainshtein & Rosner (1991) argued on theoretical grounds that one of the features fundamental to all solar cycle models, namely, the escape of dynamo-generated flux from the Sun, cannot take place at anything close to the apparent rate of emergence in ARs. Parker (1984) estimated that $\leq 3\%$ of the flux can escape. However, Parker's argument was based on much lower rates of reconnection among emerged flux ropes than seems reasonable after the evidence of the TRACE mission.

Vainshtein & Rosner (1991) accepted the possibility of coronal reconnections releasing toroidal flux, but they mistakenly assumed it could take place only above ARs. They then concluded that the coronal fields above ARs would have to average 2300 G, an unlikely value. If, however, the vehicles of flux accumulation in the corona are filaments and coronal arcades and not ARs, then Vainshtein & Rosner's (1991) reasoning would lead to an estimated average field of 23 G in the corona, in approximate agreement with observations.

Observational evidence of flux escape is accumulating. Smith & Bieber (1991) observed an apparent overwinding of the IMF and suggested it could be explained if toroidal fields escape into the solar wind. Also from IMF measurements, Bieber & Rust (1995) estimated that $\sim 10^{24}$ Mx of toroidal flux escapes the Sun per cycle and they went on to argue that CMEs and eruptive filaments could remove 100% of this toroidal flux. Smith & Phillips (1995) found that most of the IMF overwinding occurred during the periods with CMEs; that is, the fields in the CMEs account for the toroidal field in the solar wind, aside from that produced by rotation of the Sun.

In the same way that filaments with right- (left-) handed twisted fields dominate in the south (north), a like chirality segregation is also seen in the IMF (Bieber *et al.* 1987, Smith & Bieber 1993). This is an important further indication that the escaping toroids threading filaments and CMEs can be identified with the excess azimuthal component of the IMF. According to theory, the helicity of the fields should be preserved as they erupt, even if there is substantial reconnection (Taylor 1986).

Since the helicity in each hemisphere is the same for successive cycles the fields generated in a cycle cannot be canceled by oppositely directed fields from the next cycle. Helicity will accumulate in the solar atmosphere in filaments and coronal arcades until it drives them to instability and expulsion.

4. Concluding remarks

Since at least the time of the Skylab flare workshops, solar researchers have implicitly assumed that the fields in filaments could be derived from some combination of photospheric footpoint motions and reconnections in the corona. It now seems unlikely that such motions, i.e., differential rotation, meridional flow or convection, can impress the observed patterns of helicity on coronal fields. Still, an appeal to subsurface processes should be resisted, but surface motion models have been able to reproduce neither the pattern of filament field orientations nor the correct sign of helicity.

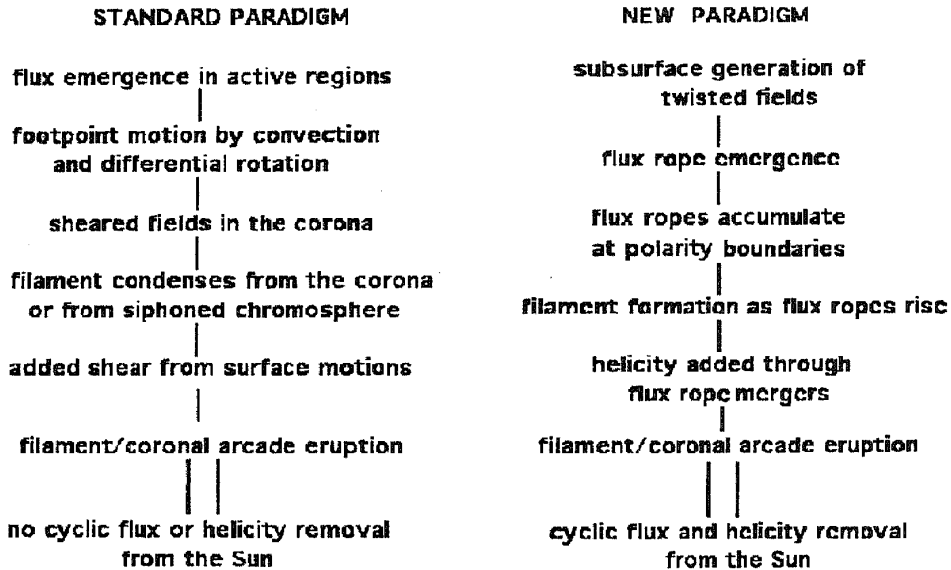


Figure 3. The new paradigm vs. the standard paradigm for filament evolution.

The new paradigm (Fig. 3) starts with some subsurface mechanism-which one(s) is not at all clear-imparting helicity to the magnetic fields before they emerge. The paradigm relies heavily on the concept of twisted flux ropes as agents of helicity transfer from the interior to the visible photosphere and subsequently to the corona.

Many of the steps between subsurface generation of twisted fields and their removal from the Sun are speculative and need to be tested by observation. Nevertheless, the new paradigm of filament formation and eruption is likely to be important in the research on the solar cycle. Magnetic flux and helicity leave the Sun in eruptive filaments and coronal mass ejections. The total flux and helicity measured in the IMF during each 11-year solar cycle is equal to the estimated total flux and helicity of the eruptives and CMEs. It is also equal to the flux and helicity in the 3000 active regions seen in a typical cycle. This is strong evidence that eruptive filaments and CMEs carry off very nearly all of the magnetic fields generated in each solar cycle.

Acknowledgements

I am grateful to Sara Martin for many interesting discussions and to J. O. Stenflo, who presented this paper when I couldn't be at the conference in person. This work was sponsored by NASA grant NAG5-7921.

References

- Amari, T., Luciani, J. F., Mikic, Z., Linker, J. 1999, *Astrophys. J.*, **518**, L57-L60.
 Athay, R. G., Querfeld, C. W., Smartt, R. N., Deglino, E. L. 1983, *Solar Phys.*, **89**, 3-30.
 Aulanier, G., Demoulin, P. 1998, *Astr. Astrophys.*, **329**, 1125-1137.
 Aulanier, G., Demoulin, P., Van Driel-Gesztelyi, L., Mein, P., Deforest, C. 1998, *Astr. Astrophys.*, **335**, 309-322.

- Babcock, H. W. 1961, *Astrophys. J.*, **133**, 572.
- Bieber, J. W., Evenson, P. A., Matthaeus, W. H. 1987, *Astrophys. J.*, **315**, 700–705.
- Bieber, J. W., Rust, D. M. 1995, *Astrophys. J.*, **453**, 911.
- Brown, M. R., Canfield, R. C., Pevtsov, A. A. (ed.) 1999, *Magnetic Helicity in Space and Lab. Plasmas*, Geophys. Monograph **111**, Amer. Geophys. U.
- Dikpati, M., Charbonneau, P. 1999, *Astrophys. J.*, **518**, 508–520.
- Gilman, P. A., Charbonneau, P. 1999, in *Magnetic Helicity in Space and Laboratory Plasmas*, Geophys. Monograph **111**, (eds.) M. R. Brown, R. C. Canfield, A. A. Pevtsov, Amer. Geophys. U., 75–82.
- Leroy, J. L., Bommier, V., Sahal-Brechot, S. 1983, *Solar Phys.*, **83**, 135–142.
- Longcope, D., Linton, M., Pevtsov, A., Fisher, G., Klapper, I. 1999, in *Magnetic Helicity in Space and Laboratory Plasmas*, (eds.) M. R. Brown, R. C. Canfield, A. A. Pevtsov, Geophys. Monograph **111**, Amer. Geophys. U., 39–101.
- Low, B. C., Hundhausen, J. R. 1995, *Astrophys. J.*, **443**, 818–836.
- Mackay, D. H., Priest, E. R., Gaizauskas, V., Van Ballegoijen, A. A. 1998, *Solar Phys.*, **180**, 299–312.
- Martin, S. F., Marquette, W. H., Bilimoria, R. 1992, in *The Solar Cycle*, (eds.) K. L. Harvey, K. L. Harvey, pp 53–66, Astron. Soc. Pacific.
- Parker, E. N. 1979, *Comical Magnetic Fields*, (Oxford: Clarendon Press).
- Parker, E. N. 1984, *Astrophys. J.*, **281**, 839.
- Pevtsov, A. A., Canfield, R. C., Metcalf, T. R. 1995, *Astrophys. J.*, **440**, L109–L112.
- Rust, D. M., Kumar, A. 1994, *Solar Phys.*, **155**, 69–97.
- Rust, D. M., Kumar, A. 1996, *Astrophys. J.*, **464**, L199–L202.
- Seehafer, N. 1990, *Solar Phys.*, **125**, 219.
- Smith, C. W., Bieber, J.W. 1991, *Astrophys. J.*, **370**, 435–441.
- Smith, C. W., Bieber, J.W. 1993, *J. Geophys. Res.*, **98**, 9401–9415.
- Smith, C. W., Phillips, J. L. 1995, *Delaware Univ., Intl. Solar Wind*, **8**, 93.
- Stix, M., 1976, in *Basic Mechanisms of Solar Activity*, *IAU Colloq.* **71**, (eds.) V. Bumba, J. Kleczek, (Reidel) 367.
- Tang, F. 1987, *Solar Phys.*, **107**, 233–237.
- Taylor, J. B. 1986, *Rev. Mod. Phys.*, **58**, 741.
- Vainshtein, S. I., Rosner, R. 1991, *Astrophys. J.*, **376**, 199.
- Van Ballegoijen, A. A., Cartledge, N. P., Priest, E. R. 1998, *Astrophys. J.*, **501**, 866.